D. L. Johnson

L. M. Schwartz

Schlumberger-Doll Research,
Old Quarry Road,
Ridgefield, CT 06877-4108

D. Elata[1]

J. G. Berryman

Earth Sciences Division,
Lawrence Livermore National Laboratory,
Mail Stop L-202,
P.O. Box 808,
Livermore, CA 94551

B. Hornby[2]

Schlumberger Cambridge Research,
High Cross,
Madingley Road,
Cambridge, CB3 0EL, UK

A. N. Norris

Department of Mechanical and
Aerospace Engineering,
Rutgers University,
Piscataway, NJ 08855-0909

Linear and Nonlinear Elasticity of Granular Media: Stress-Induced Anisotropy of a Random Sphere Pack

We develop an effective medium theory of the nonlinear elasticity of a random sphere pack based upon the underlying Hertz-Mindlin theory of grain-grain contacts. We compare our predictions for the stress-dependent sound speeds against new experimental data taken on samples with stress-induced uniaxial anistropy. We show that the second-order elastic moduli, C_{ijkl}, and therefore the sound speeds, can be calculated as unique path-independent functions of an arbitrary strain environment, $\{\epsilon_{kl}\}$, thus generalizing earlier results due to Walton. However, the elements of the stress tensor, σ_{ij}, are not unique functions of $\{\epsilon_{kl}\}$ and their values depend on the strain path. Consequently, the sound speeds, considered as functions of the applied stresses, are path dependent. Illustrative calculations for three cases of combined hydrostatic and uniaxial strain are presented. We show further, that, even when the additional applied uniaxial strain is small, these equations are not consistent with the usual equations of third-order hyperelasticity. Nor should they be, for the simple reason that there does not exist an underlying energy function which is simply a function of the current state of the strain. Our theory provides a good understanding of our new data on sound speeds as a function of uniaxial stress.

1 Introduction

Granular media exhibit a wide range of interesting properties. They are in some respects similar to solids and in other respects similar to fluids, although they are distinctly different from either. Consequently, the physics of granular media represents an active area of current research activity (Bideau and Dodds, 1991; Mehta, 1991; Nagel, 1992). A major area of interest is the manner by which applied forces are communicated from one grain to another, a subject with clear implications for the propagation of sound waves which is the topic of this article. Specifically, we present new theoretical and experimental results which clarify the way that sound speeds in granular media depend upon the applied stresses which, in general, may be anisotropic. The central issue here is that sound cannot propagate unless there is an applied stress because the "spring constants" between the grains vanish when the stress is eliminated. By measuring the effects of anisotropic stresses, we have extended earlier experimental work which had been limited to a consideration of applied stress which is strictly hydrostatic. Previous such studies are seriously inadequate, for reasons upon which we expand below.

Two related issues complicate the analysis of sound propagation in granular systems: nonlinearity and path dependence. Both effects originate with the contact forces exerted by one grain on another. Stress-induced changes in sound speeds are the fundamental signature of nonlinear elasticity. It is well known that granular media are highly nonlinear and that the rates at which sound speeds change with applied stress increase dramatically as the stress decreases. It is also known that stress versus strain experiments on such systems often show considerable hysteresis, which is due, in part, to the path-dependent nature of the contact forces. From a theoretical viewpoint, it is therefore necessary to develop nonperturbative methods of the kind employed in this paper.

We emphasize the importance of studying granular systems under the influence of anisotropic stresses. First, in conventional nonlinear *hyperelasticity* theory, there exists an energy density function which is strictly a function of the current state of strain, and not upon the past history of the deformation. Here, the so-called third-order elastic constants are used to describe the rate of change of sound speeds with applied stress or strain. (The values of the sound speeds themselves are given in terms of the second-order elastic constants, e.g., the Lamé constants λ and μ.) Even in the very simplest case of an isotropic hyperelastic medium there are three different third-order elastic constants: A, B, and C. A measurement of the change of longitudinal and of transverse sound speeds due to applied hydrostatic pressure can determine only two linearly independent combinations of these constants. Therefore, even in this simplest case, a measurement of the effects of nonhydrostatic stress is needed to complete the determination of the set A, B, C. Second, in granu-

[1] Present address: Faculty of Mechanical Engineering, Technion-I.I.T., Haifa 32000, Israel.

[2] Present address: ARCO Exp. and Prod. Tech., 2300 W. Plano Parkway, Plano, TX 75075-8499.

Contributed by the Applied Mechanics Division of THE AMERICAN SOCIETY OF MECHANICAL ENGINEERS for publication in the ASME JOURNAL OF APPLIED MECHANICS.

Discussion on the paper should be addressed to the Technical Editor, Professor Lewis T. Wheeler, Department of Mechanical Engineering, University of Houston, Houston, TX 77204-4792, and will be accepted until four months after final publication of the paper itself in the ASME JOURNAL OF APPLIED MECHANICS.

Manuscript received by the ASME Applied Mechanics Division, Mar. 19, 1997; final revision, Sept. 21, 1997. Associate Technical Editor: M. Shinozuka.

lar systems the forces exerted at the individual grain-grain contacts are path dependent. It follows that the stress-induced changes in forces are also path dependent so that sound speeds depend on the order in which stresses are applied. (This is true even though there is *no hysteresis* along any given stress path.) This issue does not arise when only hydrostatic pressure is applied nor does it arise in hyperelastic materials. Third, in geophysical applications, sedimentary rocks, which are formed from granular media, often exhibit strong acoustic anisotropy due to their inherently anisotropic stress environment (Walsh, 1965; Nur and Simmons, 1969; Nur, 1971; Lockner et al., 1977; Berryman, 1979; Helbig, 1983; Thomsen, 1986; Sayers, 1988; Sayers et al., 1990; Yin and Nur, 1992). We view the understanding of the nonlinear acoustic properties of unconsolidated granular media and the associated stress-induced anisotropy as a paradigm problem for this more general class of materials.

As the issues considered here are complicated, it will be useful to summarize the structure of this paper. In Section 2 we review the equations that describe the Hertz-Mindlin forces exerted between two grains in contact. Each contact is assumed to be rough and static friction prevents tangential slipping. In general, such forces are *not* described by a well-defined strain-energy function and any discussion of the resulting acoustic properties of the granular composite must take account of the strain history (Mindlin, 1949; Elata, 1996). Because we focus our interests here upon the role of the strain history, we employ an effective medium theory (Walton, 1987; Norris and Johnson, 1997) to make the connection between the properties of the individual grain-grain contacts and those of the composite.

We use the term "random" to distinguish our samples from ordered packings. As with all effective medium theories, only some features of the true random nature of the sample are captured by our theory, such as the average number of grain-grain contacts. This particular effective medium theory is easily generalizable to other situations, such as different bead sizes, a nonisotropic distribution of contacts, a radial distribution of contacts, but we do not explicitly consider those examples here.

Within this context, there is, surprisingly, one important relation in the acoustics of granular systems that is *path independent.* Norris and Johnson (1997) (NJ) have shown that the additional work associated with incremental displacements of a contact around a given strain state are path *independent* to second order in the *additional* strain. The coefficients of these second-order terms are, in turn, path-*independent* functions of the current state of strain. This implies that the associated equations for the second-order elastic moduli (i.e., the sound speeds) considered as functions of the strain tensor are also path *independent.* By contrast, we show that the relation between *stress* and strain is explicitly path dependent. Therefore, the sound speeds are path *independent* functions of applied strain, but path-*dependent* functions of applied stress. To illustrate these findings we consider three cases of combined hydrostatic and uniaxial strain. In Section 3 we ask if the conventional theory of third-order hyperelasticity can be used to describe this system (Hughes and Kelly, 1953; Gol'dberg, 1961). Here we show that, even when the deviations from the isotropic state are small, the path dependent nature of the forces implies that the third-order formulation is not valid, precisely because of the lack of a strain-energy function and we illustrate this point with a numerical example. In Section 4 we discuss the comparison of our analysis with new experimental results on the stress dependence of longitudinal and transverse sound speeds in a granular packing under uniaxial compression. Generally, the level of agreement between theory and experiment is quite satisfactory. Our conclusions are presented in Section 5.

2 Theory of Combined Hydrostatic and Uniaxial Strain

In this section we derive results for the elastic constants and for the stress tensor, when the strain is a combination of both hydrostatic and uniaxial compression.

2.1 Path-Dependent Contact Forces. In a recent article, Norris and Johnson (1997) considered the linear and nonlinear elasticity of different models of granular aggregates. These models differ in the nature of the grain-grain contact but can be written in the context of a common formalism. Let us suppose $2w$, $2s$ are, respectively, the normal and the transverse components of the displacement of one sphere relative to another. Let N, T be the normal and transverse components of the restoring force. An infinitesimal change in displacement ($w \to w + \Delta w$, $s \to s + \Delta s$) leads to an infinitesimal change in restoring force ($N \to N + \Delta N$, $T \to T + \Delta T$). All models considered in Norris and Johnson (1997) can be written in the form

$$\Delta N = C_n a_n(w)\Delta w, \quad \Delta T = C_t a_t(w)\Delta s, \tag{1}$$

where C_n, C_t depend only on shear modulus, μ, and the Poisson ratio, ν, of the individual grains

$$C_n = \frac{4\mu_s}{1-\nu_s}, \quad C_t = \frac{8\mu_s}{2-\nu_s}. \tag{2}$$

The quantities a_n, a_t are different for the different models of grain-grain contact but they do not depend upon the elastic constants of the grains. For the specific no-slip case being considered in the present article, one has

$$a_n(w) = a_t(w) = (Rw)^{1/2}, \tag{3}$$

where R is the radius of the spherical grain.

Let $W(w, s)$ be the work needed to displace the two grains relative to each other. In general W is very much dependent upon the path of the deformation, $s = s(w)$, and not simply upon the final values of (w, s). Suppose, however, one asks the question: How much additional work is needed to take the contact from one state characterized by (w_0, s_0) to another $(w_0 + w_1, s_0 + s_1)$? For any of the models that can be brought into the form of Eq. (1), one has the result from (Norris and Johnson, 1997)

$$W(w_0 + w_1, s_0 + s_1)$$

$$= W_0(w_0, s_0) + N_0 w_1 + T_0 s_1 + \tfrac{1}{2}C_n a_n(w_0)w_1^2 + \tfrac{1}{2}C_t a_t(w_0)s_1^2$$

$$+ \text{path-dependent third-order terms in } (w_1, s_1), \tag{4}$$

where N_0 and T_0 are the normal and transverse components, respectively, of the force between the grains at the state of displacement (w_0, s_0). The terms quadratic in w_1, s_1 are independent of the path taken in (w_1, s_1) space. Moreover, because the coefficients of these terms depend only on w_0 and not upon s_0, these terms are independent of the path of the original deformation: $s_0 = s_0(w_0)$. For this reason, the elastic constants of the ensemble of grains are well-defined functions of the current state of strain $\boldsymbol{\epsilon}$; for any of the models that can be brought to the form (1) the elastic constants can be written, in the effective medium approximation, as Eq. (60) of Norris and Johnson (1997):

$$C_{ijkl}(\boldsymbol{\epsilon}) = (1-\phi)\frac{nR^2}{4V_0}\{\langle[4C_n a_n(\xi) - 4C_t a_t(\xi)]N_i N_j N_k N_l\rangle$$

$$+ \langle C_t a_t(\xi)(\delta_{ik}N_j N_l + \delta_{il}N_j N_k + \delta_{jl}N_i N_k + \delta_{jk}N_i N_l)\rangle\}. \tag{5}$$

Here $\mathbf{N}$ is a unit vector along the sphere centers, $\xi \equiv -\mathbf{N}\cdot\boldsymbol{\epsilon}\cdot\mathbf{N}R$, $\langle\cdots\rangle$ represents an average over solid angles, n is the average number of contacts per grain, ϕ is the porosity, and $V_0 = (\frac{4}{3})\pi R^3$ is the volume of a single grain. In addition to being an effective medium approximation, Eq. (5) also presumes that the relative change in sample dimensions is negligible compared against the relative change in stiffness. For sake of numerical definiteness, we shall assume the angular distribution of contacts is isotropic, although Jenkins et al. (1989) have

argued that there is evidence of anisotropy in the distribution of contacts due to the directionality imposed by gravity.

The effective medium theory of Norris and Johnson (1997) was derived by finessing the issue of the rotation of the grains. If a symmetric strain is applied to the sample, it was pointed out that the total torque on each grain will vanish and therefore the grains will not rotate. It is therefore possible to deduce the (properly symmetrized) elastic constants and stresses as a function of the strain history. These elastic constants are the relevant ones for long-wavelength wave propagation, even, say, for shear waves. In such a motion, the grains may rotate but they do so in such a manner that the torque vanishes and the relevant elastic constants are the "torque-free" ones. See Schwartz et al. (1984) for details.

Within the effective medium framework, the validity of Eq. (5) does *not* depend on the strain history of the composite system. In the special case appropriate to Hertz-Mindlin contacts, for which Eq. (3) holds, Eq. (5) reduces to

$$C_{ijkl} = \frac{3n(1-\phi)}{4\pi^2 R^{1/2} B_W (2B_W + C_W)} \langle \xi^{1/2} \{ 2C_W N_i N_j N_k N_l + B_W (\delta_{ik} N_j N_l + \delta_{il} N_j N_k + \delta_{jl} N_i N_k + \delta_{jk} N_i N_l) \} \rangle, \quad (6)$$

where

$$B_W = \frac{2}{\pi C_n}, \quad C_W = \frac{4}{\pi}\left[\frac{1}{C_t} - \frac{1}{C_n}\right]. \quad (7)$$

Equations (6) are identical with those derived by Walton (1987) who made the unnecessary assumption that all components of the strain ϵ_{pq} are simultaneously increased together, holding their ratios fixed. We emphasize, again, that these equations are valid for any applied strain, and are independent of the history of the granular medium.

2.2 Analytic Results for Specific Strain Paths. Let us consider a special case of interest in which the strain is a combination of hydrostatic and uniaxial compression:

$$\epsilon_{ij} = \epsilon \delta_{ij} + \epsilon_3 \delta_{i3} \delta_{j3}. \quad (8)$$

2.2.1 Sound Speeds. In this case it is clear that the system will exhibit the symmetries usually associated with transversely isotropic materials and, after some rearranging, we have from Eq. (6)

$$C_{11} \equiv C_{1111} = \frac{\gamma}{\alpha}\left\{ 2B_W [I_0(\alpha) - I_2(\alpha)] + \frac{3C_W}{4}[I_0(\alpha) - 2I_2(\alpha) + I_4(\alpha)] \right\},$$

$$C_{13} \equiv C_{1133} = \frac{\gamma}{\alpha}\{ C_W [I_2(\alpha) - I_4(\alpha)] \},$$

$$C_{33} \equiv C_{3333} = \frac{\gamma}{\alpha}\{ 4B_W I_2(\alpha) + 2C_W I_4(\alpha) \},$$

$$C_{44} \equiv C_{2323} = \frac{\gamma}{\alpha}\left\{ \frac{B_W}{2}[I_0(\alpha) + I_2(\alpha)] + C_W [I_2(\alpha) - I_4(\alpha)] \right\},$$

$$C_{66} \equiv C_{1212} = \frac{\gamma}{\alpha}\left\{ B_W [I_0(\alpha) - I_2(\alpha)] + \frac{C_W}{4}[I_0(\alpha) - 2I_2(\alpha) + I_4(\alpha)] \right\}, \quad (9)$$

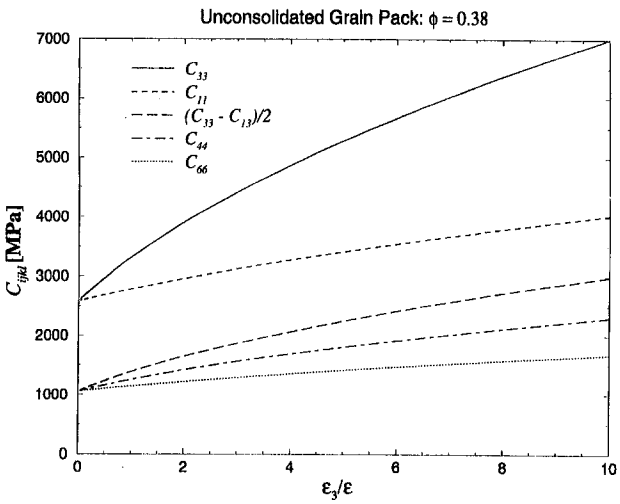

Fig. 1 The values of $\{C_{ij}\}$ are shown as functions of ϵ_3/ϵ. These are calculated from Eqs. (9) with the following parameter values: C_n = 95 GPa, C_t/C_n = 0.35, n = 6.5, ϕ = 0.38, ϵ = −0.0035.

where

$$\gamma \equiv \frac{3n(1-\phi)(-\epsilon)^{1/2}}{4\pi^2 B_W (2B_W + C_W)} = \frac{3}{32} C_n C_t n (1-\phi)(-\epsilon)^{1/2}, \quad (10)$$

$\alpha^2 \equiv \epsilon/\epsilon_3$ and $\{I_n(\alpha)\}$ denotes the integrals

$$I_n(\alpha) \equiv \int_0^1 x^n \sqrt{\alpha^2 + x^2}\, dx, \quad (11)$$

which can be evaluated analytically as

$$I_0(\alpha) = \frac{1}{2}\left[\sqrt{1+\alpha^2} + \alpha^2 \ln\left(\frac{1+\sqrt{1+\alpha^2}}{\alpha}\right)\right],$$

$$I_{2n+2}(\alpha) = \frac{1}{2n+4}[(1+\alpha^2)^{3/2} - (2n+1)\alpha^2 I_{2n}(\alpha)], \quad n \geq 0. \quad (12)$$

In Fig. 1 we show the behavior of the moduli C_{ij} calculated from Eqs. (9)–(12). The values of the parameter set were chosen in order to match our experimental data which we present later in Section 4. Instead of plotting C_{13} we show the combination $(C_{33} - C_{13})/2$ which reduces to the shear modulus, μ as $\epsilon_3/\epsilon \to 0$. (In this limit, C_{11} and C_{33} approach $\lambda + 2\mu$.) As might be expected on physical grounds, the quantity C_{33} shows the greatest variation as ϵ_3/ϵ increases. In Fig. 2 three high symmetry $(V_P/V_S)^2$ ratios are plotted against ϵ_3/ϵ. Shown also are the limiting behaviors as $\epsilon_3/\epsilon \to 0$ and $\epsilon_3/\epsilon \to \infty$. The first of the limits was discussed by Schwartz et al. (1994) within the framework of a simple perturbation expansion based on Walton's original Eq. (6). The second limit was considered by Walton, and Fig. 2 makes clear that the approach to this limiting regime is very slow. This approach is controlled by the logarithmic terms in Eqs. (12); indeed, when the results are replotted on a logarithmic scale (Fig. 3) the approach to the uniaxial limit is evident.

2.2.2 Stress Tensor. In the foregoing subsection we derived results for the second-order elastic constants as well-defined functions of the specific strain, Eq. (8). Experimentally it is difficult to monitor the strain in unconsolidated samples;

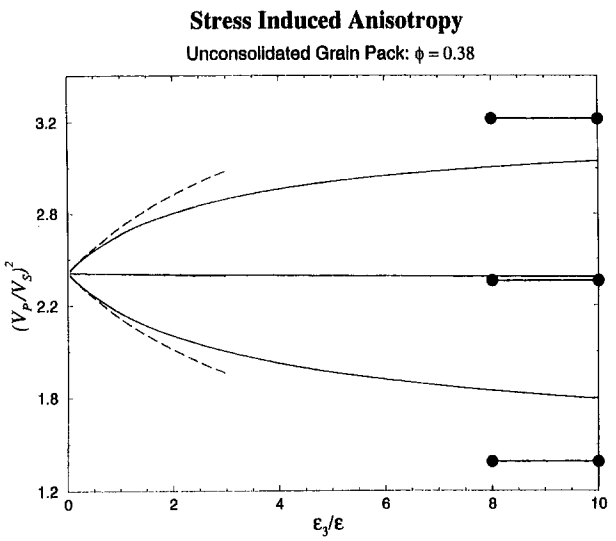

Fig. 2 Three squared sound speed ratios are plotted as functions of ϵ_3/ϵ. The upper and lower curves are the ratios C_{33}/C_{44} and C_{11}/C_{44}; the middle (nearly flat) curve is C_{11}/C_{66}. On the right-hand side the asymptotic values are shown with thick solid lines while the corresponding lines on the left-hand side give the three ratios of the initial slopes, Eqs. (27). Same parameter set as in Fig. 1.

generally it is one or more components of the stress tensor that are measured. Thus, we wish to formulate an equation relating stress to the strain elements. In order to do so, we must make a specific assumption regarding the strain history of the granular packing. In the present discussion we consider the three strain paths described in Fig. 4. In all cases the starting point is Eq. (55) of Norris and Johnson (1997), which we rewrite as

$$\sigma_{ij} = (1 - \phi)\frac{nR}{V_0}\left\{\frac{1}{2}\langle N_i T_j + N_j T_i\rangle - C_n\langle A_n(\xi)N_i N_j\rangle\right\}. \quad (13)$$

Here $\mathbf{T}$ is the path-dependent transverse force for a given contact:

$$T_i = C_t \int_{\text{path}} a_t(\xi)ds_i(\xi), \quad (14)$$

$\xi \equiv -\mathbf{N}\cdot\boldsymbol{\epsilon}\cdot\mathbf{N}R$ is the normal component of displacement, $\mathbf{s} = \mathbf{P}\boldsymbol{\epsilon}\mathbf{N}R$ is the transverse component, $\mathbf{P} = \mathbf{I} - \mathbf{NN}$ is a projection

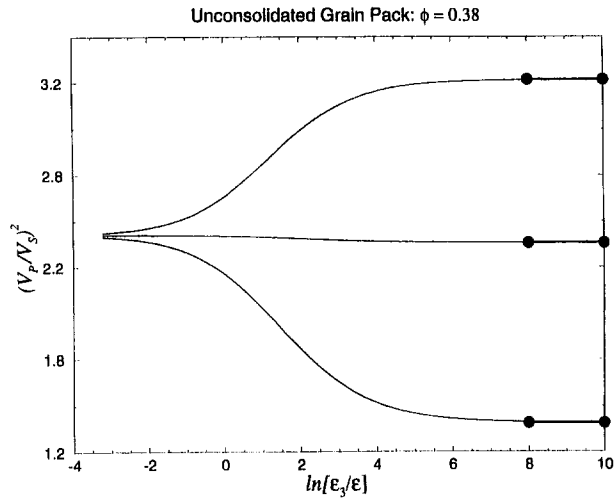

Fig. 3 The same curves shown in Fig. 2 are shown on a logarithmic scale to emphasize the slow approach to the large strain asymptote

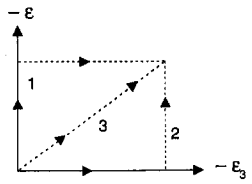

Fig. 4 Three distinct strain paths, all leading to the same final state, are illustrated schematically

operator, and $A_n(\xi) = (\frac{2}{3})R^{1/2}\xi^{3/2}$. The integral in (14) is dependent upon the path $\mathbf{s} = \mathbf{s}(\xi)$. In general, $\mathbf{T}$ and $\mathbf{s}$ are not parallel.

For the special class of deformation paths for which $\mathbf{s}$ for each contact always points in the same direction, we may write

$$\mathbf{ds} = \hat{\mathbf{s}}ds(\xi), \quad (15)$$

where $\hat{\mathbf{s}} = \mathbf{P}\boldsymbol{\epsilon}\mathbf{N}R/s$ is the (constant) unit vector in the direction of transverse displacement and $s = |\mathbf{P}\boldsymbol{\epsilon}\mathbf{N}|R$ is the magnitude of the final value of the transverse displacement. Under these restrictions, $\mathbf{T}$ and $\mathbf{s}$ are parallel and Eq. (13) becomes

$$\sigma_{ij} = (1 - \phi)\frac{nR}{V_0}\left\{C_t R\left\langle\left[\int_{\text{path}} a_t(\xi)ds(\xi)\right]\right.\right.$$
$$\left.\left.\times\frac{1}{2s}(N_i P_{jk} + N_j P_{ik})\epsilon_{kl}N_l\right\rangle - C_n\langle A_n(\xi)N_i N_j\rangle\right\}. \quad (16)$$

Let us consider path 1 in detail. Here the system is first hydrostatically compressed

$$\epsilon_{ij} = x\epsilon\delta_{ij} \quad 0 < x < 1. \quad (17)$$

Equation (17) implies $\xi = -x\epsilon R$ and $s \equiv 0$. The resulting stress is isotropic: $\sigma_{ij} = -p\delta_{ij}$ where the pressure p was first derived by Walton (1987):

$$p = -(1 - \phi)\frac{2nR^3C_n}{9V_0}(-x\epsilon)^{3/2}. \quad (18)$$

Next, an additional uniaxial compression is applied

$$\epsilon_{ij} = \epsilon\delta_{ij} + y\epsilon_3\delta_{i3}\delta_{j3}0 < y < 1. \quad (19)$$

For this path we have

$$\xi = -(\epsilon + y\epsilon_3 N_3^2)R,$$
$$s = -y\epsilon_3[N_3^2(1 - N_3^2)]^{1/2}. \quad (20)$$

At the end of this path, the deformation is that given by Eq. (8). It is straightforward to evaluate the path-dependent integrals implied by (16) as well as the angular averages. In terms of the final strain components the only nonzero stress components are σ_{33} and $\sigma_{11} = \sigma_{22}$:

$$\sigma_{33}(\epsilon, \epsilon_3) = -\frac{2(-\epsilon)^{3/2}(1 - \phi)nR^3}{3\alpha^3V_0}$$
$$\times\{C_t[\alpha^2 I_0(\alpha) + (1 - \alpha^2)I_2(\alpha) - I_4(\alpha) - 2\alpha^3/3]$$
$$+ C_n[\alpha^2 I_2(\alpha) + I_4(\alpha)]\}, \quad (21)$$

and

$$\sigma_{11}(\epsilon, \epsilon_3) = -\frac{(-\epsilon)^{3/2}(1 - \phi)nR^3}{3\alpha^3V_0}$$
$$\times\{-C_t[\alpha^2 I_0(\alpha) + (1 - \alpha^2)I_2 - I_4(\alpha) - 2\alpha^3/3]$$
$$+ C_n[\alpha^2 I_0(\alpha) + (1 - \alpha^2)I_2(\alpha) - I_4(\alpha)]\}. \quad (22)$$

In the second path described in Fig. 4, we have a uniaxial compression followed, rather than preceded, by an isotropic

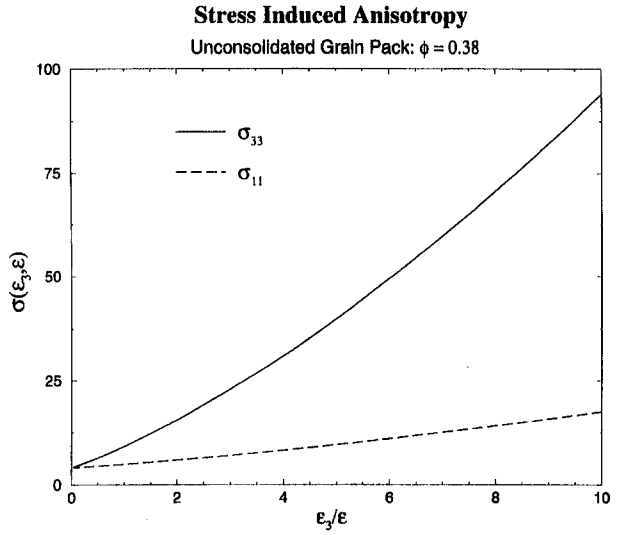

Fig. 5 The vertical and horizontal components of the stress tensor (based on Eqs. (21) and (22)) are plotted as functions of ϵ_3/ϵ. Same parameter set as in Fig. 1.

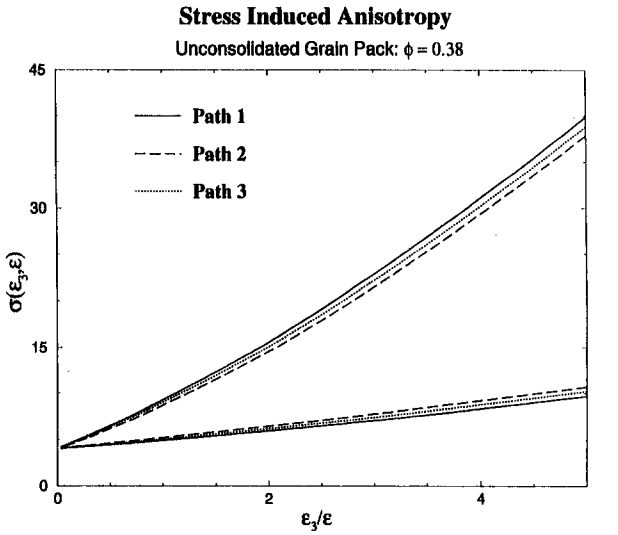

Fig. 6 The vertical and horizontal components of the stress tensor, based on the three paths shown in Fig. 4, are compared in the small strain regime. The three sets of curves remain very close for all values of ϵ_3/ϵ.

compression. The final strain configuration is the same as for path 1 but the corresponding stress is now given by

$$\sigma_{33}(\epsilon, \epsilon_3) = -\frac{2(-\epsilon)^{3/2}(1-\phi)nR^3}{3\alpha^3 V_0} \times \left\{\frac{1}{12}C_t + C_n[\alpha^2 I_2(\alpha) + I_4(\alpha)]\right\}, \quad (23)$$

and

$$\sigma_{11}(\epsilon, \epsilon_3) = -\frac{(-\epsilon)^{3/2}(1-\phi)nR^3}{3\alpha^3 V_0}\left\{-\frac{1}{12}C_t + C_n[\alpha^2 I_0(\alpha) + (1-\alpha^2)I_2(\alpha) - I_4(\alpha)]\right\}. \quad (24)$$

Finally, for the third path in Fig. 4, where the two strain components are applied simultaneously, we have

$$\sigma_{33}(\epsilon, \epsilon_3) = -\frac{2(-\epsilon)^{3/2}(1-\phi)nR^3}{3\alpha^3 V_0} \times \{C_t[I_2(\alpha) - I_4(\alpha)] + C_n[\alpha^2 I_2(\alpha) + I_4(\alpha)]\}, \quad (25)$$

and

$$\sigma_{11}(\epsilon, \epsilon_3) = -\frac{(-\epsilon)^{3/2}(1-\phi)nR^3}{3\alpha^3 V_0}\{-C_t[I_2(\alpha) - I_4(\alpha)] + C_n[\alpha^2 I_0(\alpha) + (1-\alpha^2)I_2(\alpha) - I_4(\alpha)]\}. \quad (26)$$

In each of these cases we have $\sigma_{11}(\epsilon, \epsilon_3) = \sigma_{22}(\epsilon, \epsilon_3)$. Note that the limit $\epsilon_3 \to 0$ leads to the result for hydrostatic pressure (Eq. (3.19) of Walton (1987)) and that in the opposite limit of purely uniaxial compression, $\epsilon \to 0$, the above equations all reduce to Eqs. (3.24) of Walton (1987). The stress components corresponding to the first strain path are plotted in Fig. 5. In Fig. 6, results for the different strain paths considered above are compared on an expanded scale; clearly, the differences between the three sets of curves are quite small.

3 Remarks on Third-Order Hyperelasticity Theory

Since the effective elastic constants are unique, path-independent functions of the strain tensor, it might be supposed that they are equivalent to the predictions of an effective, nonlinear hyperelastic medium. This is *not* so for the simple reason that the contact forces are path dependent, and certainly not derivable from a potential energy function. Thus the macroscopic equations of motion are not derivable from an elastic energy density function. At some point the analogy must break down. Here we demonstrate a specific contradiction between the two points of view.

It was shown in Norris and Johnson (1997) that the analogy breaks down at the third order in the expansion of the change in energy due to an incremental deformation. Although the second-order coefficients, the usual elastic constants, are path independent, the third-order terms are not. In conventional nonlinear elasticity theory, it is these third-order coefficients which determine how the sound speeds change under the application of an incremental strain applied to the system taken in some conveniently chosen reference state. Here we take the reference state to be *any* state of purely isotropic strain; this is always a valid choice for isotropic elastic systems. Let us therefore consider how the elastic constants change when a small uniaxial strain is superimposed upon a large isotropic strain, i.e., Eq. (8) to first order in ϵ_3/ϵ. It is straightforward to expand equations (9) to first order in $1/\sqrt{\alpha}$. These specific results had been reported by Schwartz et al. (1994).

$$C_{11} = \gamma\left[\frac{4B_W}{3} + \frac{2C_W}{5} + \frac{\epsilon_3}{\epsilon}\left(\frac{2B_W}{15} + \frac{C_W}{35}\right)\right],$$

$$C_{13} = \gamma\left[\frac{2C_W}{15} + \frac{\epsilon_3}{\epsilon}\left(\frac{C_W}{35}\right)\right],$$

$$C_{33} = \gamma\left[\frac{4B_W}{3} + \frac{2C_W}{5} + \frac{\epsilon_3}{\epsilon}\left(\frac{2B_W}{5} + \frac{C_W}{7}\right)\right],$$

$$C_{44} = \gamma\left[\frac{2B_W}{3} + \frac{2C_W}{15} + \frac{\epsilon_3}{\epsilon}\left(\frac{2B_W}{15} + \frac{C_W}{35}\right)\right],$$

$$C_{66} = \gamma\left[\frac{2B_W}{3} + \frac{2C_W}{15} + \frac{\epsilon_3}{\epsilon}\left(\frac{B_W}{15} + \frac{C_W}{105}\right)\right]. \quad (27)$$

Similarly, let us now consider the predictions of third-order elasticity theory for these same moduli under the same condi-

tions of small ϵ_3 but arbitary ϵ. The second and third-order elastic constants will, therefore, be seen to be functions of the isotropic strain, ϵ. Our derivation proceeds along the lines of Hughes and Kelly (1953), who considered the similar problem of the change of speeds under uniaxial *stress*; we use the Landau and Lifschitz (1986) notation as presented by Gol'dberg (1961). Thus, the second-order elastic constants are λ, μ while the third-order ones are A, B, C. Let us consider wave motion in which the propagation direction is confined to the x–z plane: $\mathbf{u} = [u(x, z), v(x, z), w(x, z)]$. We find

$$\rho_0 \frac{\partial^2 u}{\partial t^2} = C_{11} \frac{\partial^2 u}{\partial x^2} + C_{44} \frac{\partial^2 u}{\partial z^2} + (C_{13} + C_{44}) \frac{\partial^2 w}{\partial x \partial z},$$

$$\rho_0 \frac{\partial^2 w}{\partial t^2} = C_{44} \frac{\partial^2 w}{\partial x^2} + C_{33} \frac{\partial^2 w}{\partial z^2} + (C_{13} + C_{44}) \frac{\partial^2 u}{\partial x \partial z},$$

$$\rho_0 \frac{\partial^2 v}{\partial t^2} = C_{66} \frac{\partial^2 v}{\partial x^2} + C_{44} \frac{\partial^2 v}{\partial z^2}, \tag{28}$$

where (x, z) refer to the original (Lagrangian) position and, to first order in ϵ_3:

$$C_{11} = \lambda + 2\mu + \epsilon_3(\lambda + 2B + 2C),$$

$$C_{13} = \lambda + \epsilon_3(-\mu + 2B + 2C),$$

$$C_{33} = \lambda + 2\mu + \epsilon_3(3\lambda + 6\mu + 2A + 6B + 2C),$$

$$C_{44} = \mu + \epsilon_3(\lambda + 2\mu + A/2 + B),$$

$$C_{66} = \mu + \epsilon_3(\lambda + B). \tag{29}$$

Is there any way in which Eqs. (27) can be made to be equivalent to Eqs. (29)? First, we see that there is no problem with the zero-order terms which imply $\lambda = (\frac{2}{15})C_W\gamma$ and $\mu = ((\frac{2}{5})B_W + (\frac{2}{15})C_W)\gamma$. Second, the third-order constants must have a divergent term: $(A, B, C) \propto (-\epsilon)^{-(1/2)}$. Therefore, for small enough ϵ, we may neglect (λ, μ) as compared with (A, B, C) in the terms proportional to ϵ_3 because $(\lambda, \mu) \propto (-\epsilon)^{(1/2)}$. Similarly, we may neglect the distinction between the new density and the original $\rho' = (1 + \epsilon_3)\rho_0$ as well as that between the new coordinates and the old $z' = (1 + \epsilon_3)z$. There remains an unavoidable problem: If one sets the coefficient of ϵ_3 in each of Eqs. (27) equal to its counterpart in (29) (neglecting λ and μ as compared with A, B, C) we have five equations in only three unknowns. There is no set of the quantities (A, B, C) which can simultaneously satisfy these equations. This makes concrete the general demonstration that, for path-dependent contact forces, the second-order elastic constants are well-defined functions of the strain but the third-order constants are path dependent.

A careful inspection of (27) and (29) shows that the quantities dependent upon C_W can be made to match correctly but that the coefficients of B_W can not. This is a reflection of the fact that, within Walton's (1987) formulation, the normal component of stiffness for each contact is proportional to $2B_W + C_W$ whereas the tangential stiffness is proportional to $2B_W$; see Eqs. (2.13) and (2.14) of Walton (1987). It has been emphasized previously (Norris and Johnson, 1997) that the difficulty in reconciling models of path-dependent contact forces with nonlinear elasticity stems from the transverse components of the contact stiffness. Alternatively, we may say that the divergent parts of the changes in C_{ij} are predicted to obey the following relationships, according to third-order elasticity theory, Eqs. (29):

$$\Delta C_{11} - \Delta C_{13} = 0,$$

$$\Delta C_{11} + \Delta C_{33} - 2\Delta C_{13} - 4\Delta C_{44} = 0. \tag{30}$$

We see from Eqs. (27) that the second of these equations is satisfied by the predictions of the contact theory, but not the first. So to say, we have four equations (not five) in three unknowns. This is a specific manifestation of a more general property of this contact theory, derived in Norris and Johnson (1997), that changes in second-order elastic constants due to an imposed strain are governed, to first order, by four "third-order modulii," B_{111}, B_{112}, B_{123}, and $\tilde{B}$ and *not* the usual three (A, B, C).

Table 1 The quantities which determine the strain-induced anisotropy of the elastic constants for a random sphere pack, via Eqs. (27), as compared to the best fit values assuming the validity of third-order elasticity theory, equations (29). We assume $\lambda = \mu = 24$ GPa as appropriate for a silica glass. The best fit values are (ϵ/γ) $(A, B, C) = (27.2, 34.7, -17.2)$. All values in 10^{-4} $(\text{Pa})^{-1}$.

	Contact Theory		Third-Order Elasticity	
ΔC_{11}	$\left(\frac{2B_W}{15} + \frac{C_W}{35}\right)$	71.1	35.1	$\frac{\epsilon}{\gamma}(2B + 2C)$
ΔC_{13}	$\left(\frac{C_W}{35}\right)$	4.7	35.1	$\frac{\epsilon}{\gamma}(2B + 2C)$
ΔC_{33}	$\left(\frac{2B_W}{5} + \frac{C_W}{7}\right)$	222.6	228.3	$\frac{\epsilon}{\gamma}(2A + 6B + 2C)$
ΔC_{44}	$\left(\frac{2B_W}{15} + \frac{C_W}{35}\right)$	71.1	48.3	$\frac{\epsilon}{\gamma}(A/2 + B)$
ΔC_{66}	$\left(\frac{B_W}{15} + \frac{C_W}{105}\right)$	34.7	34.7	$\frac{\epsilon}{\gamma}(B)$

How serious an error might be made were one to assume the validity of third-order elasticity theory for a system such as this? Let us consider a hypothetical case of a granular medium whose strain dependent moduli are accurately given by Eq. (27) (for small ϵ_3). An experimental measurement of the change of elastic constants with uniaxial strain would be proportional to the quantities within parentheses in (27). Typical values are given in Table 1, assuming the beads are made of glass. If one were to make a best least-squares fit of Eqs. (29) to these values, the resultant values of these quantities are poorly fit by third-order elasticity theory; these values are also listed in Table 1. We see that there is an appreciable problem were one naively to apply third-order elasticity theory to the strain dependence of the sound speeds.

Winkler and Liu (1997) have already performed an experiment analogous to the *gedanken* experiment shown in Table 1. They have measured the changes in the speeds of sound as a function of applied stresses in a suite of nine rocks. They considered P and S speeds as a function of isotropic pressure and they considered P and both S speeds for waves propagating perpendicular to the axis of an applied uniaxial stress. From the initial slopes of these five measurements they determined a best fit set of values for the third-order elastic constants (A, B, C). The quality of their fit is much better than that indicated in our Table 1. Thus, we conclude that the concept of an elastic energy of deformation for sedimentary rocks may be a valid one, at least through third order in the applied strain—unlike the model of the present paper. For larger stress, though, it is known that rocks undergo hysteretic deformation (Brown et al., 1989; Hilbert et al., 1994).

4 Comparison With Experimental Data

Our measurements were made in a specialized compaction cell that was constructed to study the developing elastic properties of artificial sediments as a function of axial stress. A block diagram of the compaction cell is shown in Fig. 7. Anisotropic compressional and four-component shear wave velocities were recorded using transducers oriented parallel and perpendicular

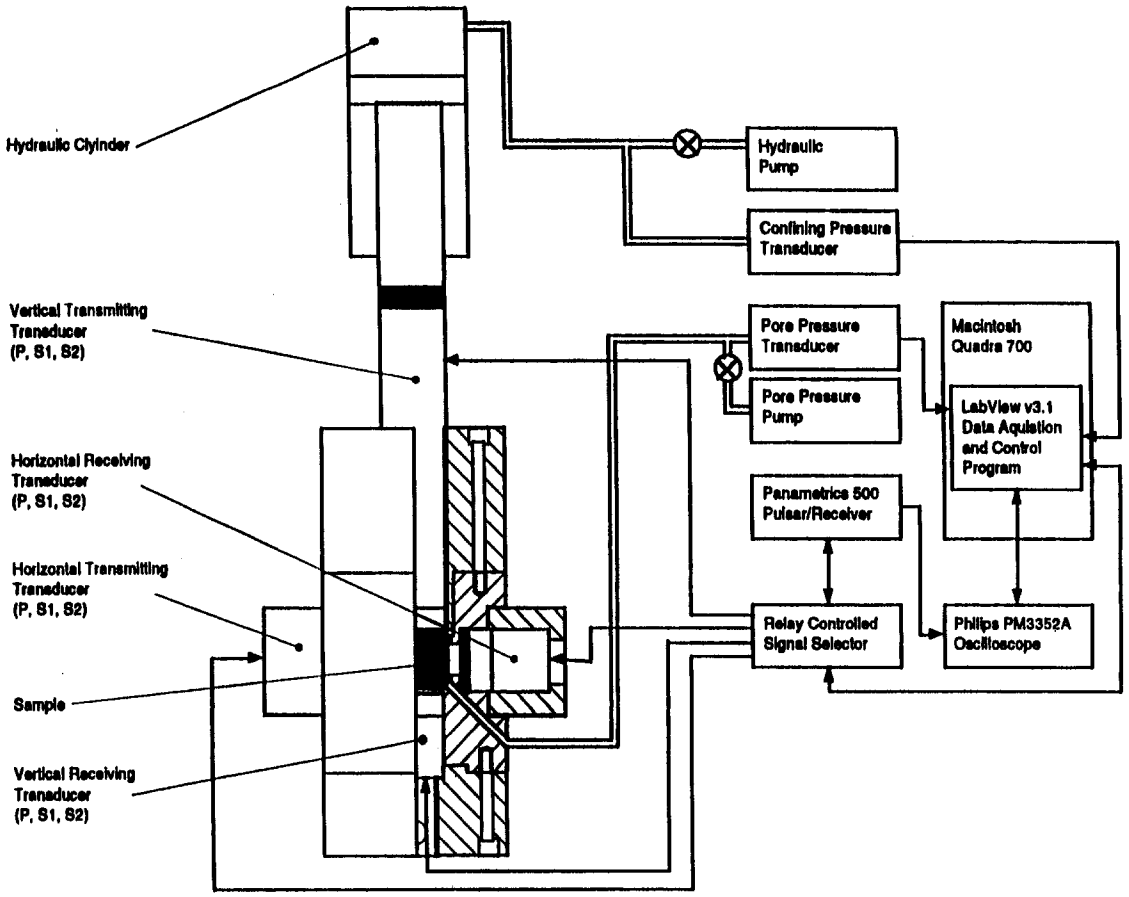

Fig. 7 Block diagram for the experimental setup used to measure the sound speeds as a function of applied stress

to the direction of axial stress. The compaction cell was constructed of EN303 stainless steel and the system has a maximum confining stress of 110 MPa. The cell is presumed to be rigid enough that the sample experiences a macroscopic uniaxial strain (negligible lateral motion). A Power Team 1826 25 ton hydraulic shop press applies the axial stress to the vertical piston. Transducers for elastic wave measurements are 4 × Verde GeoScience compressional and polarized shear wave 500 kHz ultrasonic transducers. Sample length is dynamically measured during the acquisition using a Schlumberger DC50 LVDT.

The sample we studied was comprised of dry mono-dispersed spherical glass beads with diameters of roughly 70 μm. The beads were placed in the chamber of the compaction cell and were uniaxially strained by the application of axial stresses up to 100 MPa applied over four separate cycles. To determine the P and S-wave velocities, we examined the corresponding waveforms as a function of stress for each of the four cycles. As expected, the most stable results were obtained for the last stress cycle. By this point the individual beads appear to have reached relatively stable configurations within the disordered packing. In almost all of the waveforms, the desired arrival is easily identified. However, properly locating the shear arrivals can be difficult, particularly at low applied stresses for the mode propagating normal to the direction of axial stress and polarized perpendicular to the direction of axial stress. We found that identification of weak arrivals was facilitated by examining the waveforms as a function of applied stress. While the best signal to noise ratios were obtained at the largest applied stress levels, the weaker arrivals could be identified by following the desired point of constant phase (first zero crossing) to lower stresses.

Figure 8 is a composite plot of the measured velocities for the fourth cycle of applied stress. Clearly, even for this simplest of granular media, the data show considerable hysteresis. The physical basis for this hysteresis is most likely small rearrangements in the positions of the grains during the *increasing* stress part of the cycle. Once the particles are tightly wedged together, one might assume that there are many fewer rearrangements in *decreasing* stress part of the cycle. Indeed, we believe that

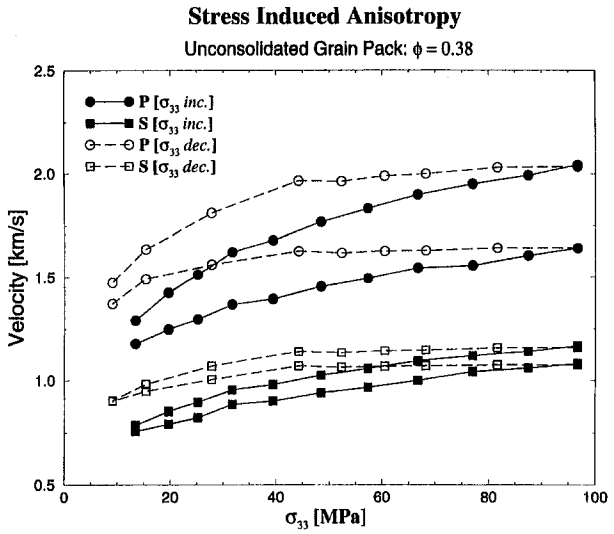

Fig. 8 Experimental results for two compressional mode (circles) and two shear mode (squares) speeds are plotted as a functions of applied vertical stress during the fourth stress cycle. The filled (open) symbols correspond to the increasing (decreasing) stress part of the cycle. The faster and slower *P* waves are associated with vertical and horizontal propagation, respectively. The faster *S* wave propagates vertically while the slower *S* wave propagates horizontally and is polarized horizontally.

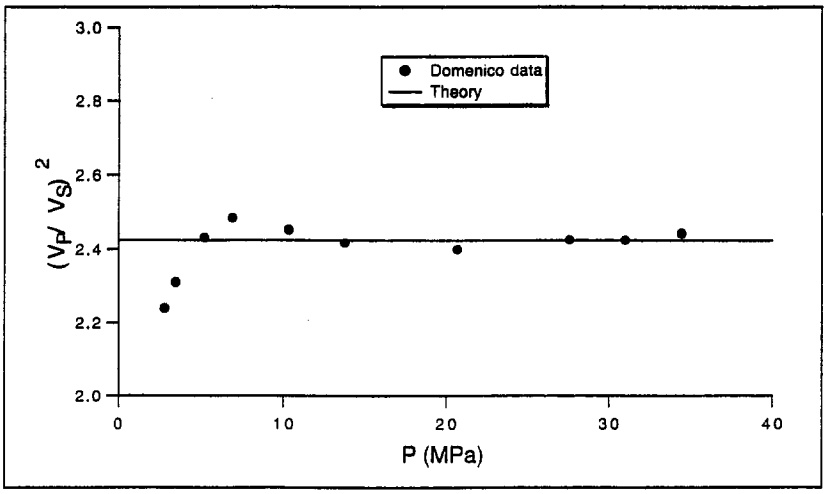

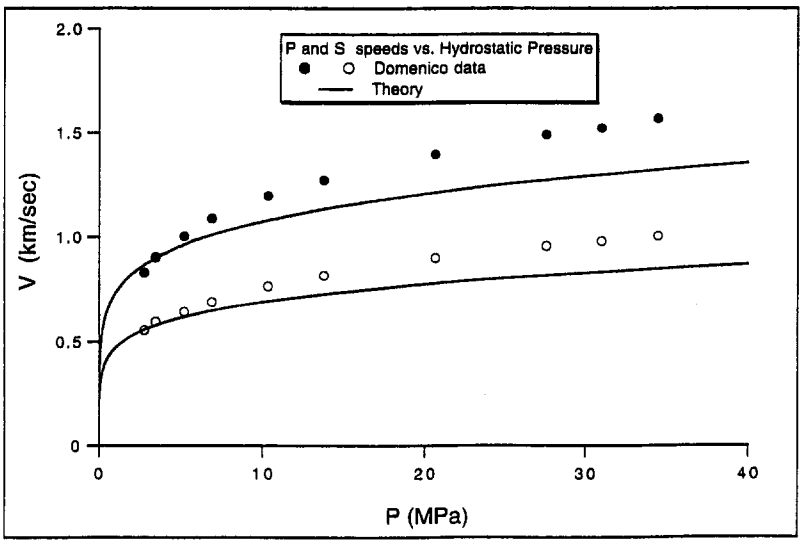

Fig. 9 V_P and V_S as a function of confining pressure for unconcolidated glass beads. The data are from Domenico (1977). The calculated value of the ratio V_P/V_S is very sensitive to the assumed value of C_t/C_n, here taken to be 0.35. The overall scale of the speeds is then set by C_n, here taken to be 95 GPa. We assume the average coordination number is n = 6.5.

this wedging of grains during the stress cycles contributes to a *residual* stress distribution in the packing even when the piston is removed and there is no applied stress. It is this residual stress that gives rise to the internal strain that we model with the parameter ϵ, the initial hydrostatic compression.

Because granular rearrangements involve breaking and reforming of contacts, they invalidate the assumption of our effective medium description of the packing. For this reason we compare our equations only with the decreasing stress part of the last cycle. To get a reasonable fit to the data we have treated the quantities n, C_n, C_t/C_n, and ϵ as adjustable parameters. We somewhat arbitrarily take n = 6.5, although only the products, nC_n and nC_t, enter in the theory. First, we demand consistency of our calculations with the data of Domenico (1977) who measured V_P and V_S as a function of *hydrostatic* confining pressure on unconsolidated glass beads. We see in Fig. 9 that the ratio V_P/V_S is essentially independent of pressure, as the theory predicts. This sets the value of the ratio C_t/C_n = 0.35. Then, the value C_n = 95 GPa was taken to ensure a reasonable overall fit to the actual speeds, as shown in Fig. 9. (For comparison, the first of Eqs. (2) yields C_n = 128 GPa and C_t/C_n = 0.857 if we take μ_s = 24 GPa and ν_s = 0.25 as appropriate for a silica glass. This would predict a value V_P/V_S that is significantly lower than the measured pressure-independent value.) Finally, the value ϵ = −0.0035 was chosen to get an acceptable fit to our own measured data. Our fit to the data is presented in Figs. 10 and 11. The calculated curves are faithful to the qualitative trends in the measured data and are in good overall agreement with the absolute values of the sound speeds and the V_P/V_S ratios. In connection with Fig. 11, we note that there is considerably less difference in the V_p/V_s ratios for the increasing and decreasing parts of the stress cycle than was seen for the absolute velocities shown in Fig. 8. We remind the reader that we have made two critical assumptions: the validity of the effective medium approximation and the assumption of no-slip between grains, either of which may be suspect. In the case of the former assumption we note that Liu et al. (1995) have given convincing theoretical and experimental arguments for the existence of a very broad (~exponential) distribution of contact forces. In the case of the latter assumption we note that our best-fit value of C_t/C_n is less than half that predicted from a literal interpretation of Eq. (2).

5 Conclusions

We have considered the elastic properties of granular media, specifically systems for which each grain-grain contact is de-

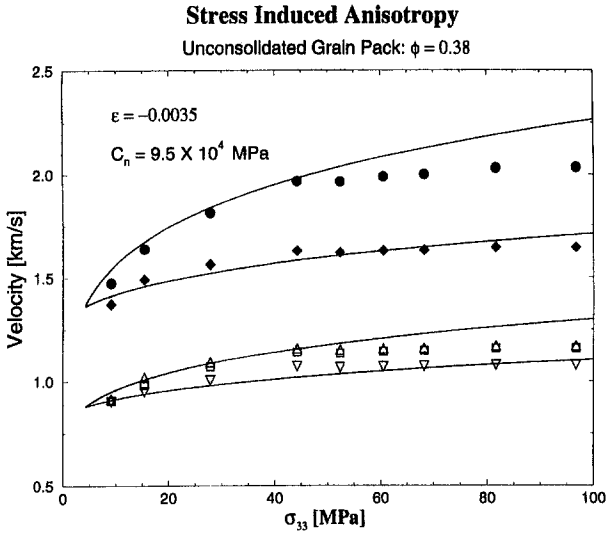

Fig. 10 The experimental speeds shown in Fig. 8 for *decreasing* applied stress are compared with the results of our calculations. Here the relation between stress and strain was calculated from Eqs. (21) and (22). Same parameter set as in Fig. 1.

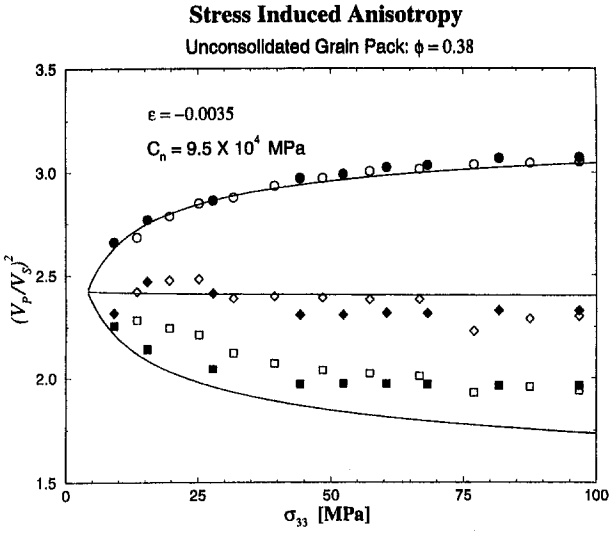

Fig. 11 Ratios of squared *P* to *S* speeds calculated as in Fig. 10 are shown together with experimental data for both the increasing and decreasing parts of the fourth stress cycle. (The relation between σ_{ij} and ϵ_{ij} is again calculated from Eqs. (21) and (22).) As in Fig. 2, the upper curve and the circles represent C_{33}/C_{44}, the middle curve and the diamonds represent C_{11}/C_{44}, and the lower curve and the squares represent C_{11}/C_{66}. In all three cases, the filled (open) symbols are the measured ratios for decreasing (increasing) stress.

scribed by a slight generalization of the Hertz-Mindlin theory. Within the context of a simple effective medium theory, we have derived expressions which describe each elastic constant as a function of a combined hydrostatic and uniaxial strain. This is a path-independent result. We have explored three different assumptions regarding the order in which the strain is applied and have calculated how the stress depends upon strain for each path. Although the second-order elastic constants are well-defined functions of the strain, the third-order constants are not. We have shown specifically how the concept of third-order elastic constants breaks down when a small uniaxial strain is applied to an unconsolidated granular medium that already has a large hydrostatic strain. Finally, we have shown how our experimental data on sound speeds measured as a function of applied stress can be understood if one assumes there is a remanent hydrostatic strain in the system.

Acknowledgments

The work of D. Elata and J. G. Berryman was performed under the auspices of the U. S. Department of Energy by the Lawrence Livermore National Laboratory under contract No. W-7405-ENG-48 and supported specifically by the Geosciences Research Program of the DOE Office of Energy Research within the Office of Basic Energy Sciences, Division of Engineering and Geosciences.

References

Berryman, J. G., 1979, "Long-wave elastic anisotropy in transversely isotropic media," *Geophysics,* Vol. 44, pp. 896–917.

Bideau, D., and Dodds, J., eds., 1991, *Physics of Granular Media,* Les Houches Series, Nova Science, Commack, NY.

Brown, E. T., Bray, J. W., and Santarelli, F. J., 1989, "Influence of Stress-Dependent Elastic Moduli on Stresses and Strains around Axisymmetric Boreholes," *Rock Mechanics and Rock Engineering,* Vol. 22, pp. 189–203.

Domenico, S. N., 1977, "Elastic properties of unconsolidated porous sand reservoirs," *Geophysics,* Vol. 42, pp. 1339–1368.

Elata, D., 1996, "On the Oblique Compression of Two Elastic Spheres," ASME JOURNAL OF APPLIED MECHANICS, Vol. 63, pp. 1039–1041.

Gol'dberg, Z. A., 1961, "Interaction of Plane Longitudinal and Transverse Elastic Waves," *Soviet Physics-Acoustics,* Vol. 6, pp. 306–310.

Helbig, K., 1983, "Elliptical anisotropy—Its significance and meaning," *Geophysics,* Vol. 48, pp. 825–832.

Hilbert, L. B., Hwong, T. K., Cook, N. G. W., Nihei, K. T., and Myer, L. R., 1994, "Effects of Strain Amplitude on the static and dynamic nonlinear deformation of Berea sandstone," *Rock Mechanics,* Nelson and Laubach, eds., Balkema, Rotterdam.

Hughes, D. S., and Kelly, J. L., 1953, "Second-Order Elastic Deformation of Solids," *Physical Review,* Vol. 92, pp. 1145–1149.

Jenkins, J. T., Cundall, P. A., and Ishibashi, I., 1989, "Micromechanical modeling of granular materials with the assistance of experiments and numerical simulations," *Powders and Grains,* Biarez and Gourvès, eds., Balkema, Rotterdam, pp. 257–264.

Landau, L. D., and Lifshitz, E. M., 1986, *Theory of Elasticity,* 3rd Ed., Pergamon, Oxford, pp. 106–107.

Liu, C.-h., Nagel, S. R., Schecter, D. A., Coppersmith, S. N., Majumdar, S., Narayan, O., and Witten, T. A., 1995, "Force Fluctuations in Bead Packs," *Science,* Vol. 269, pp. 513–515.

Lockner, D. A., Walsh, J. B., and Byerlee, J. D., 1977, "Changes in seismic velocity and attenuation during deformation of granite," *Journal of Geophysical Research,* Vol. 82, pp. 5374–5378.

Mehta, A., ed., 1991, *Granular Media: An Interdisciplinary Approach,* Springer, New York.

Mindlin, R. D., 1949, "Compliance of Elastic Bodies in Contact," ASME JOURNAL OF APPLIED MECHANICS, Vol. 71, pp. 259–268.

Mindlin, R. D., and Deresiewicz, H., 1953, "Elastic Spheres in Contact Under Varying Oblique Forces," ASME JOURNAL OF APPLIED MECHANICS, Vol. 75, pp. 327–344.

Nagel, S. R., 1992, "Instabilities in a Sandpile," *Reviews of Modern Physics,* Vol. 64, pp. 321–325.

Norris, A. N., and Johnson, D. L., 1997, "Nonlinear Elasticity of Granular Media," ASME JOURNAL OF APPLIED MECHANICS, Vol. 64, pp. 39–49.

Nur, A., and Simmons, G., 1969, "Stress-induced velocity anisotropy in rock: An experimental study," *Journal of Geophysical Research,* Vol. 74, pp. 6667–6674.

Nur, A., 1971, "Effects of stress on velocity anisotropy in rocks with cracks," *Journal of Geophysical Research,* Vol. 76, pp. 2022–2034.

Sayers, C. M., 1988, "Stress-induced ultrasonic wave velocity anisotropy in fractured rock," *Ultrasonics,* Vol. 26, pp. 311–317.

Sayers, C. M., van Munster, J. G., and King, M. S., 1990, "Stress-induced ultrasonic anisotropy in Berea sandstone," *International Journal of Rock Mechanics, Mining Science & Geomechanics Abstracts,* Vol. 27, pp. 429–436.

Schwartz, L. M., Johnson, D. L., and Feng, S., 1984, "Vibrational Modes in Granular Materials," *Physical Review Letters,* Vol. 52, pp. 831–834.

Schwartz, L. M., Murphy, W. M., and Berryman, J. G., 1994, "Stress-induced transverse isotropy in rocks," *SEG Technical Program Expanded Abstracts,* Sixty-Fourth Annual International Meeting and Exposition, p. 1081.

Thomsen, L. M., 1986, "Weak elastic anisotropy," *Geophysics,* Vol. 51, pp. 1954–1966.

Walsh, J. B., 1965, "The effects of cracks on the uniaxial elastic compression of rocks," *Journal of Geophysical Research,* Vol. 70, pp. 399–411.

Walton, K., 1987, "The effective elastic moduli of a random packing of spheres," *Journal of the Mechanics and Physics of Solids,* Vol. 35, pp. 213–226.

Winkler, K. W., and Liu, X., 1996, "Measurement of Third Order Elastic Constants in Rocks," *Journal of the Acoustical Society of America,* Vol. 100, pp. 1392–1398.

Yin, H., and Nur, A., 1992, "Stress-induced ultrasonic velocity and attenuation anisotropy of rocks," *SEG Technical Program Expanded Abstracts,* Sixty-Second Annual International Meeting and Exposition, pp. 1073–1076.